Available online at http://scik.org
Commun. Math. Biol. Neurosci. 2024, 2024:138
https://doi.org/10.28919/cmbn/8939
ISSN: 2052-2541

MODELLING THE EFFECTS OF PSYCHOLOGICAL FEAR AND VACCINATION ON THE DYNAMICS OF TYPHOID FEVER

JACKLINE WANJIKU WANGUI[1,*], MARILYN RONOH[1], CAROLINE W. KANYIRI[2], EDNA CHILENJE MANDA[3]

[1]Department of Mathematics and Statistics, University of Embu, Kenya

[2]Department of Mathematics and Actuarial Science, Catholic University of Eastern Africa, Kenya

[3]Department of Mathematics and Statistics , Mzuzu University, Malawi

Abstract. Despite the great advancements in healthcare systems and sanitary improvements globally, sub-Saharan Africa including Kenya bears a significant burden of infectious diseases, among which typhoid fever continues to exert a notable toll. In this study, we developed a deterministic mathematical model to examine the interplay between human responses driven by the psychological factor of fear of infection, vaccination efforts, and the dynamics of human-to-human and environmental transmission of typhoid fever. The mathematical model was analyzed using theories of first order ordinary differential equations to establish the existence of equilibrium points and their conditions for local and global stability. The reproduction number, $\mathscr{R}_0$, was established and distinct pathways for the transmission of infection were identified, shedding light on the crucial interactions among key population groups fueling the spread of typhoid fever disease. The model results suggests that, typhoid fever infection is heightened by both direct and indirect contact with infected individuals and contaminated environments. Additionally, lack or limited awareness contributes to decreased fear of infection and reluctance towards vaccination, further exacerbating the situation. Moreover, an increase in environmental transmission is observed due to elevated discharge rates from infected individuals. This study contributes valuable insights into the design of effective mitigation strategies aimed at combating typhoid fever in resource-limited settings.

*Corresponding author

E-mail address: wjackline755@gmail.com

Received October 03, 2024

Keywords: typhoid fever; modelling; vaccination; psychological factor; fear.

2020 AMS Subject Classification: 92D30.

1. INTRODUCTION

Typhoid fever continues to present a global hazard, resulting in over 21 million infections and 200,000 fatalities annually [1]. The disease is particularly endemic in sub-Saharan Africa, with about 400,000 incidences annually and a high mortality rate of about 0.762% [2]. The high rates of morbidity and mortality associated with this infection can be partially attributed to the emergence and the spread of drug-resistant *Salmonella Typhi* bacteria, fueled by the widespread use of second-generation antibiotics such as ciprofloxacin and levofloxacin, which diminishes the efficacy of these antibiotics against this pathogen [3]. In sub-Saharan Africa, including Kenya, a significant proportion of the population resides below the poverty line, inhabiting densely populated areas characterized by poor sanitation and heightened exposure to infected individuals and contaminated environments [4]. These crowded spaces often lack adequate sanitation facilities, leaving vulnerable demographics, such as infants and school-ongoing children, particularly susceptible to adverse health effects from typhoid fever infection and other infectious diseases [5].

Typhoid fever is endemic in Kenya, with approximately 126,000 incidences reported every year and frequent outbreaks observed in central, coastal and western parts of Kenya [6]. Most of these outbreaks were traced to limited access to clean water sources, inadequate latrines, and poor hygiene facilities, particularly among street food vendors and their clients [6]. Notably, in early 2023, Kenya reported an outbreak at one local secondary school in Western Kenya involving 1062 patient cases, predominantly students, which resulted in a number of mortality cases [7]. The outbreak was attributed to contaminated food, poor personal hygiene and untreated water [7]. In most developing countries, prevention and control of typhoid fever disease include drinking treated water, proper sanitation, vaccination and adequate medical care [8].

Recent advancements in vaccination have contributed greatly to reduced incidences of typhoid fever globally [2]. However, widespread rollout of typhoid fever vaccine as a routine tool for disease prevention in many endemic regions in sub-Saharan Africa continues to face

significant hurdles [9]. Lack of adequate knowledge about typhoid fever vaccine, declining efficacy of typhoid fever vaccines over time, insufficient funding to support widespread vaccine rollout due to government priorities, inadequate health infrastructure, cultural and religious beliefs, community norms, vaccine hesitancy fueled by misinformation and distrust in healthcare systems are some of the factors hindering the uptake and efficacy of typhoid fever vaccines in endemic regions [10]. In addition, accessibility and affordability present significant challenges in sub-Saharan Africa, with vaccines potentially inaccessible due to cost or logistical hurdles [11]. Implementing effective and affordable strategies is urgently required in most affected and high-risk populated areas to effectively control typhoid fever in resource-limited regions [12].

To further aid the understanding of typhoid fever dynamics, novel tools such as mathematical models have been employed to provide key insights influencing the spread of this disease and forecast potential interventions for effectively mitigating the disease [13, 14, 15, 16]. Very few of these studies considered a combination of psychological factor of fear of infection and vaccination as control strategies. Historically, human behavior have been intricately linked to the dynamics of infectious diseases and therefore their understanding is key for effective control and management of infectious diseases such as typhoid fever [17]. Hence, this study aims to investigate the effect of the psychological factor of fear of infection combined with vaccination in the transmission dynamics of typhoid fever while taking into account the direct and indirect modes of transmission. This study seeks to contribute valuable insights into the design of effective mitigation strategies aimed at combating typhoid fever in resource-limited settings.

The paper is organized as follows. In section 2 we define the model properties. In section 3 we conduct mathematical analysis to establish the disease-free equilibrium point and endemic equilibrium point along with conditions for their local and global stability. Additionally, we present the reproduction number and its biological interpretations. In section 4, we estimate the model parameters and utilize them to perform numerical simulations of the system. Section 5 provides discussion and conclusion of the study.

2. MODEL FORMULATION

We develop a mathematical model to examine the interplay between human responses driven by the psychological factor of fear of infection and vaccination efforts in the transmission dynamics of typhoid fever. This formulation takes into account both direct and indirect modes of typhoid fever transmission. The direct mode of typhoid fever transmission occurs through human-to-human contact via the fecal-oral route whereas the indirect transmission takes place when a susceptible individual ingests contaminated water or food that has been contaminated with *Salmonella typhi* bacteria typically sewage-contaminated water or food handled by an infected person [6].

We categorize the human population into four classes such that at time $t \geq 0$ there are susceptible individuals $(S(t))$, infected individuals stemming from direct transmission resulting from human - human interaction (I_h), infected humans stemming from indirect transmission resulting from human interaction with contaminated environment (I_e) and the recovered individuals (R) following treatment. We also include the class B, which represents the bacteria population in the environment. The total size of the human of the human population is given as $N_h(t) = S(t) + I_h(t) + I_e(t) + R(t)$ and the total size of both the human and bacteria populations $N(t)$ is given as $N(t) = S(t) + I_h(t) + I_e(t) + R(t) + B(t)$.

The susceptible class (S) is free from typhoid fever infection, but when in contact with infected individuals (I_h, I_e) or contaminated environments, they are at risk of typhoid fever infection at the incidence rates β_h, β_e, resulting from the direct and indirect modes of transmission, respectively. The expressions for β_h, β_e are given as follows:

$$\beta_h = \frac{(1-\psi_f)C_h(\eta_1 I_h + \eta_2 I_e)}{N_h},\ \beta_e = \frac{C_e(1-\psi_f)B}{K+B}$$

where C_h, C_e denotes effective contact rate for typhoid fever transmission to occur for direct and indirect transmission, respectively. The parameters η_1 and η_2 represent the veracity of infection from infected individuals with *Salmonella Typhi* bacteria, with $\eta_1 < \eta_2$, given that the probability of typhoid fever transmission for a susceptible individual in contact with an infected individual is lower compared to when a susceptible individual is in contact with a contaminated

environment [14]. Thus, η_1, η_2 are dimensionless parameters to differentiate the severity of the typhoid fever infection.

Parameter ψ_f represents the psychological factor of fear of infection which drives individuals to improve their sanitation, personal hygiene and exercise care during meal preparations or purchasing food. We let $0 < \psi_f < 1$ where $\psi_f = 0$ implies that there is no dread to typhoid fever disease either due to lack of awareness or simply negligence and this significantly increases the contact rate which in turn fuels the spread of typhoid fever. $\psi_f = 1$ implies that individuals are fully aware of the typhoid disease spread and its controls due to effective education campaigns. In this case, individuals are fully adherent to preventive measures and are fully aware of the consequences of neglecting sanitation and personal hygiene. Thus, fear of contracting the typhoid fever disease drives them to significantly limit any contact rate with possible sources of contamination and this reduces the spread of typhoid fever disease significantly. The behavioral dynamics can be linked to more immediate reactions in an emerging epidemic. The impact on disease dynamics might be extremely substantial if protective behavioral changes brought about by fear of contracting the disease is significantly high in the community. When people are self-aware of the disease and maintain proper sanitation, the disease is significantly reduced. However, numerous waves of infection may result from their later re-entry into the population when their dread fades.

The parameter K represents the carrying capacity of *Salmonella Typhi* bacteria in the environment such as water or food due to limited resources to sustain its growth indefinitely. $\frac{B}{B+K}$ represents the fraction of the carrying capacity K that is currently occupied by the bacteria population B in the environment. In this formulation, recruitment rate into the *Salmonella Typhi* bacteria population is described by a logistic growth equation b, given as $b = rB(1 - \frac{B}{K})$ where r represents per capita growth rate of the bacteria population. The bacteria population is cleared from the environment at a rate τ.

Parameter α represents the proportion of the susceptible individuals who are vaccinated against typhoid fever disease. This study assumes that vaccination is a continuous process. Given that typhoid fever vaccination does not confer 100% protection against typhoid fever

infection, the vaccinated population can become susceptible when the vaccination loses its efficacy, thus $0 < \alpha < 1$. $\alpha = 1$ represents an ideal scenario where a highly efficacious typhoid fever vaccine guarantees permanent immunity against typhoid fever disease, whereas when $\alpha = 0$, implies that the susceptible population is not vaccinated.

Susceptible class (S) is increased by natural birth λ and the recovered population that lose immunity at a rate ω from the recovered class and is reduced by the newly infected individuals that move to the infected classes I_h and I_e as a result of the incidence rates $\rho(1-\alpha)\beta_h$ and $(1-\rho)(1-\alpha)\beta_e$ respectively. Parameter ρ represents the proportion of newly infected individuals as a result of contact with humans to humans interaction (direct mode) whereas $1-\rho$ represents newly infected individuals as a result of humans to environment interaction (indirect mode). Infected classes I_h and I_e are increased by the incidence rates $\rho(1-\alpha)\beta_h$ and $(1-\rho)(1-\alpha)\beta_e$ and all are decreased by the death due to infection δ and recovery rate ε. The Recovered class (R) increases due to the newly recovered individuals at a rate ε, and decreases due to individuals losing their immunity at a rate ω, who then return to the susceptible class. Populations, S, I_h, I_e, R are further reduced to natural deaths at a natural death rate μ.

Tables 1 and 2 provide a summary description for the state variables and parameters used in the typhoid fever model respectively. The schematic diagram presented in figure 1 describes the transmission dynamics of typhoid fever in the human and bacteria populations.

TABLE 1. Description of State Variables

Variables	Description
S	Susceptible human population at time t
I_h	Infected human resulting from direct transmission at time t
I_e	Infected human resulting from indirect transmission at time t
R	Recovered human population at time t
B	Bacteria concentration in the environment at time t

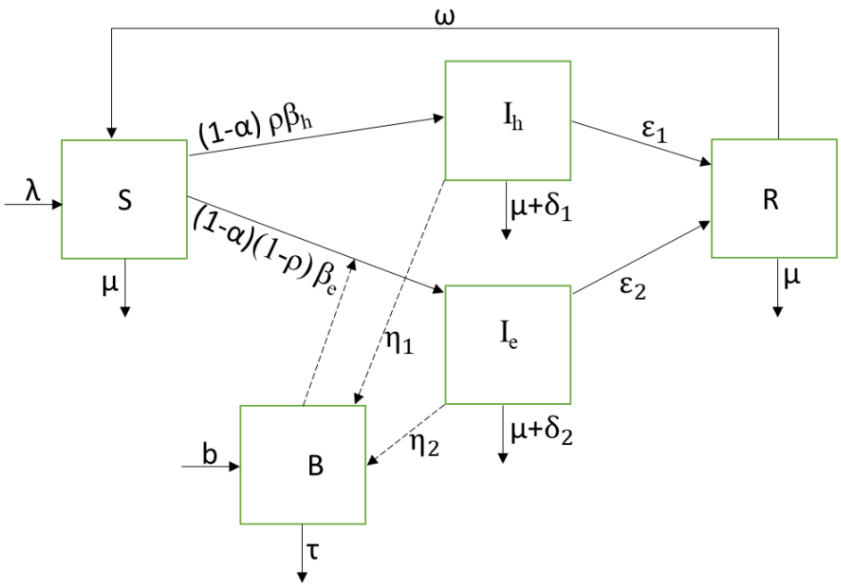

FIGURE 1. Typhoid Fever Model

$$\frac{dS}{dt} = \lambda - [(\rho\beta_h + (1-\rho)\beta_e)(1-\alpha) + \mu]S + \omega R. \tag{1}$$

$$\frac{dI_h}{dt} = \rho\beta_h(1-\alpha)S - (\mu + \delta_1 + \varepsilon_1)I_h. \tag{2}$$

$$\frac{dI_e}{dt} = (1-\rho)(1-\alpha)\beta_e S - (\mu + \delta_2 + \varepsilon_2)I_e. \tag{3}$$

$$\frac{dR}{dt} = \varepsilon_1 I_h + \varepsilon_2 I_e - (\mu + \omega)R. \tag{4}$$

$$\frac{dB}{dt} = b + \eta_1 I_h + \eta_2 I_e - \tau B. \tag{5}$$

TABLE 2. Description of Parameters

Parameter	Description
λ	Recruitment rates into the susceptible populations through natural births
μ	Natural death rate of individuals
ψ_f	Psychological factor of fear of typhoid fever infection
ω	Rate at which the recovered individuals lose immunity
ε_1	Rate of newly recovered individuals from I_h
ε_2	Rate of newly recovered individuals from I_e
η_1	Dimensionless parameter representing veracity of typhoid fever infection when contact is between susceptible and I_h
η_2	Dimensionless parameter representing veracity of typhoid fever infection when contact is between susceptible and I_e
α	Proportion of vaccinated susceptible Individuals
δ_1	Disease induced death rates stemming from I_h
δ_2	Disease induced death rates stemming from I_e
ρ	Proportion of newly infected individuals due to direct transmission mode
τ	Clearance rate of the bacteria in the environment
r	Per capita growth rate of the bacteria population in the environment
K	Carrying capacity for the bacteria
C_h	Effective contact rate with infected humans
C_e	Effective contact rate with contaminated environment

3. Model Analysis

3.1. Positivity of Solutions. We show that if all the trajectories starts with non-negative initial conditions, the solutions will remain non-negative for all $t \in (0,\infty)$. We thus consider the following theorem;

Theorem 1. *Let* $R = (S, I_h, I_e, R, B) \in R_+^5 : S_0 > 0, I_{h0} > 0, I_{e0} > 0, R_0 > 0, B_0 > 0$,*; then the solutions of* $R = (S, I_h, I_e, R, B)$ *are positive for all* $t \geq 0$.

Proof. To show positivity of solutions we, let S, I_h, I_e, R and B be a solution of the system with non-negative initial conditions. From the system of nonlinear differential equations, we consider equation (1); The first term λ and the last term ωR are positive by inspection method.

$$\frac{dS(t)}{dt} \geq -[(\rho\beta_h + (1-\rho)\beta_e)(1-\alpha) + \mu]S(t). \tag{6}$$

The resulting differential inequality is solved by separation of variables method.

$$S(t) \geq \exp - \int_0^t [(\rho\beta_h + (1-\rho)\beta_e)(1-\alpha) + \mu]dt \exp c \tag{7}$$

Applying the initial condition, let $t = 0$ we have,

$$S(t) = S(0)\exp -[(\rho\beta_h + (1-\rho)\beta_e)(1-\alpha) + \mu]t \geq 0. \tag{8}$$

Similarly, using the same procedure, the rest state variables from equations (2)-(5) can be shown to satisfy as shown.

$$I_h(t) \geq I_{h0}\exp -(\mu + \delta_1 + \varepsilon_1)t \geq 0. \tag{9}$$

$$I_e(t) \geq I_{e0}\exp -(\mu + \delta_2 + \varepsilon_2)t \geq 0. \tag{10}$$

$$R(t) \geq R_0 \exp -(\mu + \omega)t \geq 0. \tag{11}$$

$$B(t) \geq \tau B_0 \exp - \tau t \geq 0. \tag{12}$$

This completes the proof of the theorem. Therefore, we conclude that the solutions of the model are non-negative. □

3.2. Boundedness of Solutions. The model is separated into two sections which include, the human population T_H and the concentration of the bacteria in the environment T_B such that $T_H = (S(t), I_h(t), I_e(t), R(t)) \in \mathbb{R}^4_+ : S + I_h + I_e + R = N$. and $T_B = B(t) \in \mathbb{R}^1_+$. respectively.

We consider boundedness of solutions of system equations (1)-(4) at time t given as

$$N_h(t) = S(t) + I_h(t) + I_e(t) + R(t). \tag{13}$$

Differentiating equation (13)gives

$$\frac{dN_h}{dt} = \frac{dS}{dt} + \frac{dI_h}{dt} + \frac{dI_e}{dt} + \frac{dR}{dt}. \tag{14}$$

Substituting equations (1)-(4) in equation (14) we have

$$\frac{dN_h}{dt} = \lambda - \mu N_h - \delta I. \tag{15}$$

In absence of no infectious human with typhoid fever disease ($\delta = 0$), equation (15) becomes

$$\frac{dN_h}{dt} \leq \lambda - \mu N_h(t). \tag{16}$$

Using method of separation of variables of inequality, we have

$$-\frac{1}{\mu}\ln(\lambda - \mu N_h(t)) \leq t + c.$$

$$\lambda - \mu N_h(t) \geq De^{-\mu t}. \tag{17}$$

Solving equation (17) and evaluating as $t \to \infty$, we have

$$\lim_{t\to\infty} N_h(t) = \frac{\lambda}{\mu}. \tag{18}$$

Implying that,

$$0 \leq N_h(t) \leq \frac{\lambda}{\mu}. \tag{19}$$

Therefore, the model is bounded in the domain.

$$T_H = (S, I_h, I_e, R) \in \mathbb{R}^4_+ : 0 \leq N_h(t) \leq \frac{\lambda}{\mu}.$$

We then consider the boundedness of solution for the bacteria concentration at time t from equation (5), we have

$$\frac{dB}{dt} = b + \eta_1 I_h + \eta_2 I_e - \tau B.$$

$$\frac{dB}{dt} + \tau B = b + \eta_1 I_h + \eta_2 I_e. \tag{20}$$

Let $M = b + \eta_1 I_h + \eta_2 I_e$. which is the rate at which bacteria from infectious groups are recruited. Thus, we obtain a differential inequality

$$\frac{dB}{dt} + \tau B \leq M. \tag{21}$$

Using integration factor method

$$I.F = e^{\int \tau dt}.$$

$$I.F = e^{\tau t}. \tag{22}$$

Multiplying equation (21) by equation (22) on both sides we have

$$e^{\tau t} B' + e^{\tau t} \tau B = M e^{\tau t}. \tag{23}$$

Thus,

$$B \leq \frac{M}{\tau} + C e^{-\tau t}. \tag{24}$$

Where C is a constant. Thus, as $t \to \infty$, we have

$$\lim_{t \to \infty} B(t) = \frac{M}{\tau}. \tag{25}$$

Which implies that

$$0 \leq B(t) \leq \frac{M}{\tau}. \tag{26}$$

$$T_B = B(t) \in \mathbb{R}^1_+ : 0 \leq B(t) \leq \frac{M}{\tau}.$$

Thus the domain of biological significance of the typhoid fever model is

$$T = \left[(S, I_h, I_e, R, B) \geq 0 : N_h(t) \leq \frac{\lambda}{\mu}; B(t) \leq \frac{M}{\tau} \right].$$

The domain T is bounded and positively invariant.

3.3. Disease-Free Equilibrium (DFE). We qualitatively analyze the stability of the steady states in absence of typhoid fever that is $I_h = I_e = B = 0$. To obtain the DFE, we set the right-hand side of the model differential equations (1)-(5) to zero which on solving results to

$$S_0 = \frac{\lambda}{\mu}. \tag{27}$$

On solving equations (2)-(5) the result is zero. Thus, the disease-free equilibrium E_0 becomes

$$E_0 = \left(\frac{\lambda}{\mu}, \quad 0, \quad 0, \quad 0, \quad 0\right). \tag{28}$$

3.4. Reproduction Number ($\mathscr{R}_0$). The reproduction number $\mathscr{R}_0$ is the average number of secondary infections caused by an infectious individual in his or her entire period of infectiousness in a completely susceptible population. In this study, we compute the $\mathscr{R}_0$ using the next generation matrix method described in [18]. The reproduction number is a key quantity measure in the disease epidemiology as it is a determining factor of whether the disease persists or die out in a given population. When $\mathscr{R}_0 > 1$, it indicates that each infected person is typically causing more than one secondary infection thus the epidemic the disease invades the population. In contrast, the disease is likely to die out when $\mathscr{R}_0 < 1$, since an infected individual typically infects fewer people. We define matrix FV^{-1} as

$$FV^{-1} = \left[\frac{\partial \mathscr{F}_i(E_0)}{\partial x_j}\right]\left[\frac{\partial \mathscr{V}_i(E_0)}{\partial x_j}\right]^{-1},$$

where matrix $\mathscr{F}_i$ represents the rate of appearances of new infections in compartment i, Matrix $\mathscr{V}_i$ represent the transfer of infections from one compartment i to another and E_0 is the disease-free equilibrium.

Infection matrix $\mathscr{F}_i$ and transition matrix $\mathscr{V}_i$ are given as follows

$$\mathscr{F}_i = \begin{pmatrix} \rho(1-\psi_f)C_h(\eta_1 I_h)(1-\alpha) + \rho(1-\psi_f)C_h(\eta_2 I_e)(1-\alpha) \\ \frac{(1-\rho)(1-\psi_f)C_e B(1-\alpha)\lambda}{(K+B)\mu} \\ 0 \end{pmatrix},$$

$$\mathscr{V}_i = \begin{pmatrix} (\mu+\delta_1+\varepsilon_1)I_h \\ (\mu+\delta_2+\varepsilon_2)I_e \\ \tau B - rB(1-\frac{B}{K}) - \eta_1 I_h - \eta_2 I_e \end{pmatrix}.$$

Differentiating $\mathscr{F}_i$ and $\mathscr{V}_i$ with respect to I_h, I_e and B at E_0 we obtain F and V as

$$F = \begin{pmatrix} \rho(1-\psi_f)C_h(\eta_1)(1-\alpha) & \rho(1-\psi_f)C_h(\eta_2)(1-\alpha) & 0 \\ 0 & 0 & \frac{(1-\alpha)(1-\rho)(1-\psi_f)C_e\lambda}{K\mu} \\ 0 & 0 & 0 \end{pmatrix},$$

$$V = \begin{pmatrix} \mu+\delta_1+\varepsilon_1 & 0 & 0 \\ 0 & \mu+\delta_2+\varepsilon_2 & 0 \\ -\eta_1 & -\eta_2 & \tau-r \end{pmatrix}.$$

The inverse matrix of V, denoted V^{-1} is given as

$$V^{-1} = \begin{pmatrix} \frac{1}{\mu+\delta_1+\varepsilon_1} & 0 & 0 \\ 0 & \frac{1}{\mu+\delta_2+\varepsilon_2} & 0 \\ \frac{\eta_1}{(\mu+\delta_1+\varepsilon_1)(\tau-r)} & \frac{\eta_2}{(\mu+\delta_2+\varepsilon_2)(\tau-r)} & \frac{1}{\tau-r} \end{pmatrix}.$$

Computing, FV^{-1} we have

$$FV^{-1} = \begin{bmatrix} \frac{\rho(1-\psi_f)C_h\eta_1(1-\alpha)}{(\mu+\delta_1+\varepsilon_1)} & \frac{\rho(1-\psi_f)C_h\eta_2(1-\alpha)}{(\mu+\delta_2+\varepsilon_2)} & 0 \\ \frac{(1-\alpha)(1-\rho)(1-\psi_f)C_e\eta_1\lambda}{(\mu+\delta_1+\varepsilon_1)(\tau-r)\mu} & \frac{(1-\alpha)(1-\rho)(1-\psi_f)C_e\eta_2\lambda}{(\mu+\delta_2+\varepsilon_2)(\tau-r)\mu} & \frac{(1-\alpha)(1-\rho)(1-\psi_f)C_e\lambda}{K(\tau-r)\mu} \\ 0 & 0 & 0 \end{bmatrix}.$$

The basic reproduction number, $\mathscr{R}_0$, is the spectral radius of FV^{-1} which is given by the dominant eigenvalue value of the next generation matrix.

To find the eigenvalues, we first consider the following conventions to simplify the expressions in the matrix FV^{-1}.

$$R_1 = \frac{\rho(1-\psi_f)C_h\eta_1(1-\alpha)}{(\mu+\delta_1+\varepsilon_1)},$$
$$R_2 = \frac{\rho(1-\psi_f)C_h\eta_2(1-\alpha)}{(\mu+\delta_2+\varepsilon_2)},$$
$$R_3 = \frac{(1-\alpha)(1-\rho)(1-\psi_f)C_e\eta_1\lambda}{(\mu+\delta_1+\varepsilon_1)(\tau-r)\mu},$$
$$R_4 = \frac{(1-\alpha)(1-\rho)(1-\psi_f)C_e\eta_2\lambda}{(\mu+\delta_2+\varepsilon_2)(\tau-r)\mu},$$
$$R_5 = \frac{(1-\alpha)(1-\rho)(1-\psi_f)C_e\lambda}{K(\tau-r)\mu}.$$

Computing the eigenvalues yields the following

$$\lambda_1 = 0.$$
$$\lambda_2 = \frac{1}{2}(R_4 + R_1 - \sqrt{(R_4 - R_1)^2 + 4R_2R_3}).$$
$$\lambda_3 = \frac{1}{2}(R_4 + R_1 + \sqrt{(R_4 - R_1)^2 + 4R_2R_3}).$$

Where λ_3 is the dominant eigenvalue with $R_4 \geq R_1$. The reproduction number $\mathscr{R}_0$ for typhoid fever model system described in equations (1)-(5) is given in equation (29) as

$$R_0 = \frac{1}{2}(R_4 + R_1 + \sqrt{(R_4 - R_1)^2 + 4R_2R_3}). \tag{29}$$

R_1 and R_2 represent the average number of newly infected individuals through direct mode of typhoid fever transmission whereas R_5 represents the average number of newly infected individuals through indirect modes. R_3 and R_4 represent the average number of newly infected individuals through both direct and indirect modes. This implies that R_1, represents the average number of newly infected individuals resulting from interactions between susceptible population and infected population I_h only whereas R_2 stems from interactions between susceptible population and infected population I_e only. R_5 represents average number of newly infected population when interaction only occurs between a susceptible population and contaminated environment. R_3 stems from interactions between susceptible population and infected population I_h as well as contaminated environment. Similarly, R_4 results from interactions between a susceptible population and infected population I_e as well as contaminated environment.

3.5. Local stability of Disease-Free Equilibrium (DFE). We analyze the stability of the disease free equilibrium point qualitatively. From the model system:

Theorem 2. *Model system* (1)-(5) *is locally asymptotically stable if* $R_0 < 1$.

Proof. We apply the Routh Hurwitz Criterion [19], which states that given a polynomial of degree 3, $P(\lambda) = \lambda^3 + a_1\lambda^2 + a_2\lambda + a_3 = 0$ and the corresponding Hurwitz Matrix is given as

$$Q = \begin{vmatrix} a_1 & 1 & 0 \\ a_3 & a_2 & a_1 \\ 0 & 0 & a_3 \end{vmatrix}.$$

To verify if the Disease free equilibrium point is locally stable using the Routh Hurwith criterion, we need to show that the determinant, $det(Q) = a_3(a_1a_2 - a_3) > 0$ and that, $a_1 > 0, a_3 > 0$ and $a_1a_2 > a_3$.

To get Matrix Q we subtract matrix F and Matrix V, that is

$$F-V = \begin{pmatrix} \rho(1-\psi_f)C_h(\eta_1)(1-\alpha) & \rho(1-\psi_f)C_h(\eta_2)(1-\alpha) & 0 \\ 0 & 0 & \frac{(1-\alpha)(1-\rho)(1-\psi_f)C_eS_0}{K} \\ 0 & 0 & 0 \end{pmatrix} - \begin{pmatrix} \mu+\delta_1+\varepsilon_1 & 0 & 0 \\ 0 & \mu+\delta_2+\varepsilon_2 & 0 \\ -\eta_1 & -\eta_2 & \tau-r \end{pmatrix}.$$

Thus,

$$F-V = \begin{pmatrix} a-d & b & 0 \\ 0 & -e & c \\ -f & -g & -h \end{pmatrix}.$$

To find the characteristic equation we find

$$|(F-V)-\lambda I| = 0$$

$$(F-V)-\lambda I = \begin{bmatrix} a-d & b & 0 \\ 0 & -e & c \\ -f & -g & -h \end{bmatrix} - \begin{bmatrix} \lambda & 0 & 0 \\ 0 & \lambda & 0 \\ 0 & 0 & \lambda \end{bmatrix} = \begin{bmatrix} a-d-\lambda & b & 0 \\ 0 & -e-\lambda & c \\ -f & -g & -h-\lambda \end{bmatrix}$$

$$|(F-V)-\lambda I| = \begin{vmatrix} a-d-\lambda & b & 0 \\ 0 & -e-\lambda & c \\ -f & -g & -h-\lambda \end{vmatrix} = 0.$$

Thus, we have,

$$a-d-\lambda \begin{vmatrix} e-\lambda & c \\ -g & -h-\lambda \end{vmatrix} - b \begin{vmatrix} 0 & c \\ -f & -h-\lambda \end{vmatrix} + 0 \begin{vmatrix} 0 & -e-\lambda \\ -f & -g \end{vmatrix} = 0.$$

Thus, the characteristic equation becomes,

$$P(\lambda) = -\lambda^3 + (a-d-e-h)\lambda^2 + (ae+ah-de-dh-eh-cg)\lambda + aeh + acg - deh - dcg - bcf = 0.$$

From the Routh Hurwitz stability criterion, the characteristic equation becomes,

$$P(\lambda) = \lambda^3 - (a-d-e-h)\lambda^2 - (ae+ah-de-dh-eh-cg)\lambda - aeh - acg + deh + dcg + bcf = 0.$$

Thus, comparing this characteristic equation with the general form of Routh Hurwitz stability criterion, we have,

$$a_1 = d+e+h-a$$

$$a_2 = de+dh+eh+cg-ae-ah$$

$$a_3 = deh+dcg+bcf-aeh-acg$$

Thus, the Hurwitz matrix becomes,

$$Q = \begin{vmatrix} d+e+h-a & 1 & 0 \\ deh+dcg+bcf-aeh-acg & de+dh+eh+cg-ae-ah & d+e+h-a \\ 0 & 0 & deh+dcg+bcf-aeh-acg \end{vmatrix}.$$

$$\det Q = deh+dcg+bcf-aeh-acg((d+e+h-a)(de+dh+eh+cg-ae-ah) - (deh+dcg+bcf-aeh-acg)) > 0.$$

Therefore, according to Routh Hurwitz, the following conditions are satisfied.

$$a_1 = d+e+h > a.$$

$$a_3 = deh+dcg+bcf > aeh+acg.$$

$$a_1a_2 = ea^2+a^2h+2ed^2+d^2h+3edh+ecg+dh^2+eh^2+cdg-acg-2ead- 2adh-3eah-ah^2-e^2a > a_3.$$

Thus, since, $\det Q > 0, a_1 > 0, a_3 > 0,$ and, $a_1 a_2 > a_3$ then the disease free equilibrium point is locally stable. □

Where

$$a = \rho(1-\psi_f)C_h(\eta_1)(1-\alpha).$$

$$b = \rho(1-\psi_f)C_h(\eta_2)(1-\alpha).$$

$$c = \frac{(1-\alpha)(1-\rho)(1-\psi_f)C_e S_0}{K}.$$

$$d = \mu + \delta_1 + \varepsilon_1.$$

$$e = \mu + \delta_2 + \varepsilon_2.$$

$$f = \eta_1.$$

$$g = \eta_2.$$

$$h = \tau - r.$$

3.6. Global Stability of the DFE. To determine the global stability of the DFE, the Castillo-Chavez method is applied [20, 21]. We consider the following theorem:

Theorem 3. *Point* $P = (X^*, 0) = (\frac{\lambda}{\mu}, 0, 0, 0, 0)$ *is globally stable* $\iff R_0 < 1$ *and that conditions* $(H1)$ *and* $(H2)$ *are satisfied in the system* (1)-(5).

Proof. Thus, the system in the reduced form gives:

$$\begin{cases} \dfrac{dX}{dt} = F(X,Z), \\ \dfrac{dZ}{dt} = G(X,Z), G(X,0) = 0. \end{cases}$$

Where X represent the population not infected while Z represent the infected population.

And $E_0 = (X,0), P = (X^*,0) = (\frac{\lambda}{\mu}, 0, 0, 0, 0)$ represents the disease free equilibrium state of the system.

To guarantee the global asymptotic stability, the following conditions must also satisfy

$$(H1) : \frac{dX}{dt} = F(X^*, 0), X^* \text{is globally asymptotic stable.}$$

$$(H2) : G(X,Z) = AI - G(X,0) \geq 0 \text{ for } (X,Z) \in \mathbb{R}^2_+ \text{where} A = D_1 G(X^*, 0).$$

A is the Metzler matrix that is, the domain where the model is well-posed and makes biological sense is the non-negative off diagonal element of A. And this implies that the fixed point $E_0 = (X^*, 0)$ has a global asymptotic stability point of the model provided $R_0 < 1$. Thus, for the condition $(H1)$ to be satisfied we have

$$F(X,0) = \begin{pmatrix} \lambda - [(\rho\beta_h + (1-\rho)\beta_e)(1-\alpha) + \mu]S + \omega R \\ \varepsilon_1 I_h + \varepsilon_2 I_e - (\mu+\omega)R \end{pmatrix}.$$

for the equilibrium state $E_0 = (X^*, 0)$ the systems yields the following,

$$\frac{dX}{dt} = \lambda - [(\rho\beta_h + (1-\rho)\beta_e)(1-\alpha) + \mu]S + \omega R.$$
$$\frac{dX}{dt} = \varepsilon_1 I_h + \varepsilon_2 I_e - (\mu+\omega)R.$$

Which implies that,

$$F(X,0) = \begin{pmatrix} -[(\rho\beta_h + (1-\rho)\beta_e)(1-\alpha) + \mu] & \omega \\ 0 & -(\mu+\omega) \end{pmatrix}.$$

If we let $w = (\rho\beta_h + (1-\rho)\beta_e)(1-\alpha)$, thus, to determine the characteristic polynomial we apply the following

$$F(X,0) - \lambda I = \begin{pmatrix} -(w+\mu) & \omega \\ 0 & -(\mu+\omega) \end{pmatrix} - \begin{pmatrix} \lambda & 0 \\ 0 & \lambda \end{pmatrix} = 0.$$

Implying that,

$$\begin{vmatrix} -(w+\mu) - \lambda & \omega \\ 0 & -(\mu+\omega) - \lambda \end{vmatrix} = 0.$$

Thus, the characteristic equation of the polynomial becomes

$$\lambda^2 + (3\omega + w)\lambda + 2(w+\omega)\omega = 0. \tag{30}$$

According to the Routh-Hurwitz criterion, solutions to the characteristic polynomial contain negative real components as all of the characteristic polynomials in equation (30) are non-negative. Thus suggests that the real parts of the eigenvalues are negative. As a result, X^* is globally asymptotic stable.

Furthermore, for $(H2)$ to be satisfied, that is : $G(X,Z) = AI - G(X,0)$.

$$G(X,Z) = \begin{pmatrix} -(\mu+\delta_1+\varepsilon_1) & 0 & 0 \\ 0 & -(\mu+\delta_2+\varepsilon_2) & 0 \\ \eta_1 & \eta_2 & r-\tau \end{pmatrix}.$$

Thus,$G(X,Z) = AI - G(X,0)$ becomes;

$$\begin{pmatrix} -(\mu+\delta_1+\varepsilon_1) & 0 & 0 \\ 0 & -(\mu+\delta_2+\varepsilon_2) & 0 \\ \eta_1 & \eta_2 & r-\tau \end{pmatrix} \begin{pmatrix} I_h \\ I_e \\ B \end{pmatrix} - \begin{pmatrix} (\rho\beta_h(1-\alpha)S \\ (1-\rho)\beta_e(1-\alpha)S \\ 0 \end{pmatrix}.$$

Since A is a Metzler matrix, and that as $t \to \infty$, $(I_h, I_e, B) \to (0,0)$. Therefore,$F(X,Z) \geq 0$ and since the two conditions are satisfied the Disease Free Equilibrium is Globally Asymptotically Stable in R. □

3.7. Endemic Equilibrium point.

Lemma 4. *For $\mathscr{R}_0 > 1$, there exists a unique endemic equilibrium point at E^* otherwise it does not exist.*

Proof. To determine the endemic equilibrium point that is $E^* = (S^*, I_h^*, I_e^*, R^*, B^*)$, we equate the systems of differential equation for the states S, I_h, I_e, R, B to zero to estimate the endemic equilibrium points for both the human and bacteria populations.

Determining the endemic equilibrium for the human population that is, $E_h^* = (S_h^*, I_h^*, I_e^*, R_h^*)$ we let,

$$a_1 = \rho(1-\alpha),$$

$$a_2 = (1-\rho)(1-\alpha),$$

$$a_3 = \mu + \delta_1 + \varepsilon_1,$$

$$a_4 = \mu + \delta_2 + \varepsilon_2,$$

and let β_h^* and β_e^* be equilibrium points such that

$$\beta_h^* \leq \frac{(1-\psi_f)C_h(\eta_1 I_h^* + \eta_2 I_e^*)}{N_h^*},$$

$$\beta_e^* \leq \frac{C_e(1-\psi_f)B^*}{K+B^*}.$$

Thus, computing the endemic equilibrium for the human population yields

$$S_h^* \approx \frac{a_2a_3a_4\lambda}{a_1a_2a_3a_4\beta_h^* - a_1a_3\omega\beta_h^*\varepsilon_1 + a_2^2a_3a_4\beta_e^* - a_2^2\omega\beta_e^*\varepsilon_2 + a_2a_3a_4\mu} > 0,$$

$$I_h^* \approx \frac{\lambda(a_1a_3\beta_h^*\varepsilon_1) + a_2^2\beta_e^*\varepsilon_2}{a_1a_2a_3a_4\beta_h^* - a_1a_3\omega\beta_h^*\varepsilon_1 + a_2^2a_3a_4\beta_e^* - a_2^2\omega\beta_e^*\varepsilon_2 + a_2a_3a_4\mu} > 0,$$

$$I_e^* \approx \frac{a_1\beta_h^*a_3a_4\lambda}{a_1a_2a_3a_4\beta_h^* - a_1a_3\omega\beta_h^*\varepsilon_1 + a_2^2a_3a_4\beta_e^* - a_2^2\omega\beta_e^*\varepsilon_2 + a_2a_3a_4\mu} > 0,$$

$$R_h^* \approx \frac{a_2^2\beta_e^*a_4\lambda}{a_1a_2a_3a_4\beta_h^* - a_1a_3\omega\beta_h^*\varepsilon_1 + a_2^2a_3a_4\beta_e^* - a_2^2\omega\beta_e^*\varepsilon_2 + a_2a_3a_4\mu} > 0.$$

Calculating the endemic equilibrium for bacteria population we let b^* be an endemic equilibrium point such that

$$b^* \leq rB^*\left(1 - \frac{B^*}{K}\right).$$

Therefore,

$$\begin{aligned} b^* + \eta_1 I_h^* + \eta_2 I_e^* - \tau B &\geq 0, \\ rB(K-B) + \eta_1 K I_h^* + \eta_2 K I_e^* - \tau BK &\geq 0, \\ KrB - rB^2 - \tau BK + \bar{\eta}K(I_h^* + I_e^*) &\geq 0. \end{aligned}$$

$$-rB^2 + BK(r-\tau) + \bar{\eta}K(I_h^* + I_e^*) \geq 0. \tag{31}$$

Let

$$\begin{aligned} q_1 &= K(r-\tau), \\ q_2 &= \bar{\eta}K(I_h^* + I_e^*). \end{aligned}$$

Solving the quadratic equation given in (31), the endemic equilibrium point for the bacteria population is approximated as follows

$$B^* \leq \frac{q_1 + \sqrt{q_1^2 + 4rq_2}}{2r}.$$

□

3.8. Global Stability of Endemic Equilibrium. To study the global asymptotic stability of the endemic equilibrium point, we apply the LaSalle's invariance principle.

Theorem 5. *The endemic equilibrium point E^* of a system is globally asymptotically stable when $\mathscr{R}_0 > 1$.*

Proof. We employ the LaSalle's invariance principle to prove the global stability of the endemic eqilibrium point. We use the following lyapunov function.

$$V(S,I_h,I_e,R,B) \leq \left(S - S^* + S^* \ln \frac{S}{S^*}\right) + \left(I_h - I_h^* + I_h^* \ln \frac{I_h}{I_h^*}\right) + \left(I_e - I_e^* + I_e^* \ln \frac{I_e}{I_e^*}\right) + \left(R - R^* + R^* \ln \frac{R}{R^*}\right) + \left(B - B^* + B^* \ln \frac{B}{B^*}\right).$$

Differentiating V with respect to t we have

(32)
$$\frac{dV}{dt} \leq \left(1 - \frac{S^*}{S}\right)\frac{dS}{dt} + \left(1 - \frac{I_h^*}{I_h}\right)\frac{dI_h}{dt} + \left(1 - \frac{I_e^*}{I_e}\right)\frac{dI_e}{dt} + \left(1 - \frac{R^*}{R}\right)\frac{dR}{dt} + \left(1 - \frac{B^*}{B}\right)\frac{dB}{dt}.$$

Replacing the values of $\frac{dS}{dt}, \frac{dI_h}{dt}, \frac{dI_e}{dt}, \frac{dR}{dt}, \frac{dB}{dt}$ in the equation (32) we get

$$\begin{aligned}\frac{dV}{dt} \leq{}& \left(1 - \frac{S^*}{S}\right)(\lambda - [(\rho\beta_h + (1-\rho)\beta_e)(1-\alpha) + \mu]S + \omega R) + \\ & \left(1 - \frac{I_h^*}{I_h}\right)(\rho\beta_h(1-\alpha)S - (\mu + \delta_1 + \varepsilon_1)I_h) + \\ & \left(1 - \frac{I_e^*}{I_e}\right)((1-\rho)(1-\alpha)\beta_e S - (\mu + \delta_2 + \varepsilon_2)I_e) + \left(1 - \frac{R^*}{R}\right)(\varepsilon_1 I_h + \varepsilon_2 I_e - (\mu + \omega)R) + \\ & \left(1 - \frac{B^*}{B}\right)\left(rB(1 - \frac{B}{K})\right) + \eta_1 I_h + \eta_2 I_e - \tau B.\end{aligned}$$

Which implies,

$$\begin{aligned}\frac{dV}{dt} \leq{}& \lambda + \omega R - ((\rho\beta_h + (1-\rho)\beta_e)(1-\alpha) + \mu)S - (\lambda + \omega R)\frac{S^*}{S} + \\ & (\rho\beta_h(1-\alpha) + (1-\rho)(1-\alpha)\beta_e + \mu)S^* + \rho\beta_h(1-\alpha)S - (\mu + \delta_1 + \varepsilon_1))I_h - \\ & (\rho\beta_h(1-\alpha)S)\frac{I_h^*}{I_h} + (\mu + \delta_1 + \varepsilon_1))I_h^* + (1-\rho)(1-\alpha)\beta_e S - (\mu + \delta_2 + \varepsilon_2)I_e -\end{aligned}$$

$$(1-\rho)(1-\alpha)\beta_e S\frac{I_e^*}{I_e}+(\mu+\delta_2+\varepsilon_2)I_e^*+\varepsilon_1 I_h+\varepsilon_2 I_e-(\mu+\omega)R-(\varepsilon_1 I_h+\varepsilon_2 I_e)\frac{R^*}{R}+$$
$$(\mu+\omega)R^*+\left(rB(1-\frac{B}{K})\right)+\eta_1 I_h+\eta_2 I_e-\tau_B-\left(rB(1-\frac{B}{K})\right)\frac{B^*}{B}-(\eta_1 I_h+\eta_2 I_e)\frac{B^*}{B}+\tau_B^*.$$

Collecting the positive terms and negative terms together gives

$$\frac{dV}{dt}\leq\lambda+(\rho\beta_h(1-\alpha)+(1-\rho)(1-\alpha)\beta_e+\mu)S^*+(\mu+\delta_1+\varepsilon_1)I_h^*+(\mu+\delta_2+\varepsilon_2)I_e^*+$$
$$\varepsilon_1 I_h+\varepsilon_2 I_e+(\mu+\omega)R^*+\left(rB(1-\frac{B}{K})\right)+\eta_1 I_h+\eta_2 I_e+\tau_B^*-(\lambda+\omega R)\frac{S^*}{S}-$$
$$(\mu+\delta_1+\varepsilon_1))I_h-(\rho\beta_h(1-\alpha)S)\frac{I_h^*}{I_h}-(\mu+\delta_2+\varepsilon_2)I_e-(1-\rho)(1-\alpha)\beta_e S\frac{I_e^*}{I_e}-\mu R-$$
$$(\varepsilon_1 I_h+\varepsilon_2 I_e)\frac{R^*}{R}-\tau_B-\left(rB(1-\frac{B}{K})\right)\frac{B^*}{B}(\eta_1 I_h+\eta_2 I_e)\frac{B^*}{B}.$$

Setting Q to represent the positive terms and W to represent the negative terms we have

$$\frac{dV}{dt}\leq Q-W.$$

If $Q<W$, then $\frac{dV}{dt}\leq 0$;

Note that, $\frac{dV}{dt}\leq 0$ if and only if $S=S^*, I_h=I_h^*=I_e=I_e^*, R=R^*, B=B^*$.

Thus, the largest compact invariant set in $(S^*,I_h^*,I_e^*,R^*,B^*)\in\mathbb{R}_+^5:\frac{dV}{dt}\leq 0$ is the singleton E^* where E^* is the endemic equilibrium of the system (1)-(5).

From the Lassalle's invariant principle it shows that E^* is globally asymptotically stable $\mathbb{R}_+^5$ if $Q<W$. □

4. NUMERICAL SIMULATION

4.1. Parameter Estimation. This section details how the initial data and parameter values used for the model simulations were obtained. We calibrated the model using demographic data from Kisii County in Kenya because most parameter values were estimated from a typhoid fever study [22] conducted there. The model can be applicable to various regions that share similar dynamics as this study, provided they fall within the parameter range of this research. Other parameter values were obtained from the weekly bulletin on typhoid fever outbreaks [7]. Using demographic data from Kisii town in Kenya, we estimated the initial susceptible population to be approximately 130,000 [22]. Additionally, we used the Kenyan demographic data to

calculate parameter values for recruitment and death rates. The average lifespan of a Kenyan is 67 years [23]. To estimate the death rate, we shall take the reciprocal of the average life expectancy, that is, $\mu = \frac{1}{67} = 0.01493$. In 2023, approximately 4% of deaths were attributed to typhoid fever in Kenya [7]. Hence, we estimate the disease induced death rate $\delta_1 = \frac{4}{100} = 0.04$. We calculate the recruitment rate into the susceptible class using the expression for the state of the model at the disease free equilibrium point, $S_0 = \frac{\lambda}{\mu}$, which yields, $\lambda = \mu S_0 = 0.01493. \times 130000 = 1941$.

All parameters used in model analysis and numerical simulation are given in Table 3.

TABLE 3. Parameter Values

Parameter	Value	Unit	Source
λ	1941	year^{-1}	Calculated
μ	0.01493	year^{-1}	Calculated
ψ_f	varied(0-1)	-	
ω	0.33	year^{-1}	[13]
ε_1	0.0625	year^{-1}	[22]
ε_2	0.0625	year^{-1}	[22]
η_1	varied(0-1)	-	
η_2	varied(0-1)	-	
α	varied(0-1)	-	
δ_1	0.0400	year^{-1}	Calculated
δ_2	0.0503	year^{-1}	Estimated
ρ	0.5	year^{-1}	[24]
τ	0.0007	year^{-1}	Estimated
r	0.00001	year^{-1}	Estimated
K	500000	year^{-1}	[14]
C_h	0.1533	year^{-1}	[13]
C_e	0.8133	year^{-1}	Estimated

4.2. Numerical Results. Numerical simulations were conducted to explore the evolution of the transmission dynamics of typhoid fever disease taking into account the direct and indirect modes of transmission alongside the efficacy of control measures such as vaccination and the psychological factor of fear. Using the parameter values given in table 3 we simulated the

model system for equations (1)-(5) with initial states given as $S = 130,000, I_h = 1265, I_e = 9442, R = 5000$,and the initial state for the bacteria population $B = 145707$. The parameters for the psychological factor of fear ψ_f, vaccination α, and discharge rates (η_1, η_2) were varied from a baseline value of 0 to a maximum value of 1, in order to determine their impact on the transmission dynamics. Figure 2 shows the modelling outcomes when psychological factor of fear ψ_f and vaccination are either varied, ranging from a low rate of 0 to a high efficacy rate of 1, high efficacy rate of 1, or fixed at a low baseline rate of 0.1 and a high rate of 0.9 respectively. Meanwhile, key parameters are varied to observe their effects on the modelling outcomes.

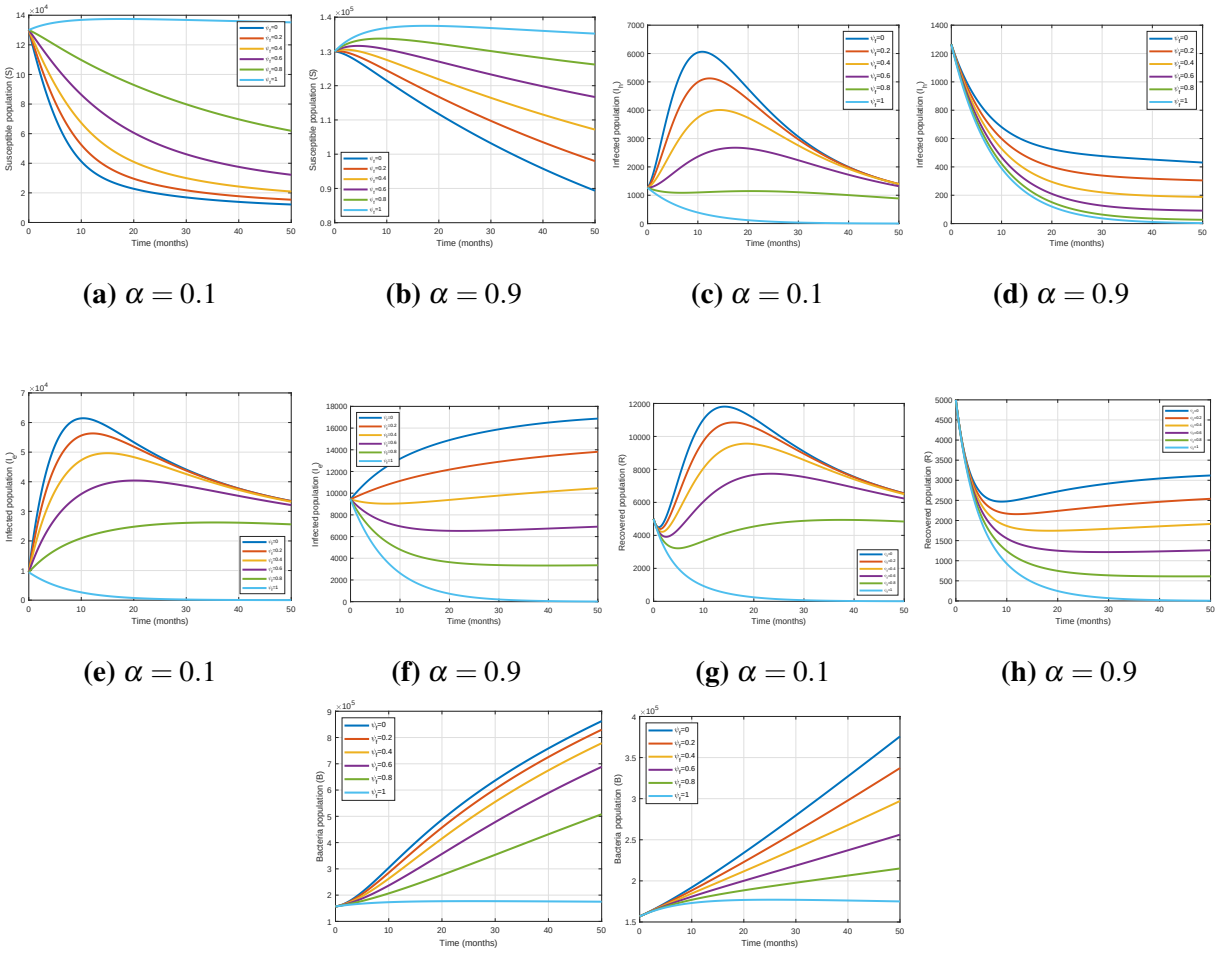

(a) $\alpha = 0.1$ **(b)** $\alpha = 0.9$ **(c)** $\alpha = 0.1$ **(d)** $\alpha = 0.9$

(e) $\alpha = 0.1$ **(f)** $\alpha = 0.9$ **(g)** $\alpha = 0.1$ **(h)** $\alpha = 0.9$

(i) $\alpha = 0.1$ **(j)** $\alpha = 0.9$

Figure 2. Effects of varying ψ_f on both human and bacteria populations when α is fixed at 0.1 and 0.9 respectively

Figures 2a-2j show the effects of varying ψ_f, on both human and bacteria populations when α is fixed at low baseline rate of 0.1 and a high efficacy rate of 0.9 respectively. The susceptible population decreases significantly when the psychological factor of fear, ψ_f, is low, and decreases even further when paired with low vaccination rates (see figures 2a–2b). However, when the psychological factor of fear is high, specifically within the range of 0.9 to 1, even with low vaccination rates, fewer susceptible individuals become infected with typhoid fever. Better results are achieved when both vaccination and the psychological factor of fear are sustained between 0.9 and 1. The number of infected populations is significantly decreased with steady increase in psychological factor of fear, ψ_f, from 0 to 1 (see figures 2c–2f). Similarly, recovered populations, R, are further reduced with an increase in ψ_f (see figures 2g–2h). Figures 2i-2j, show that, the bacteria concentration is reduced by high rates of ψ_f. Better results are achieved when psychological factor of fear, ψ_f and vaccination rates, α are both steadily increased to high efficacy rates.

Figures 3a-3h show the effects of varying η_1 and η_2, on both human and bacteria populations when α and ψ_f are fixed at rate of 0.5 . The susceptible population decreases significantly when the discharge rates η_1 and η_2 are high (see figures 3a–3b) even when paired with the psychological factor of fear and vaccination, ψ_f and α, fixed at 0.5. The number of infected populations is significantly increased with steady increase in η_1 and η_2 from 0 to 1 (see figures 3c–3d). Similarly, recovered populations, R, are increased with an increase in η_1 and η_2 (see figures 3e–3f). Figures 3g–3h, show that, the bacteria concentration is reduced by low rates of η_1 and η_2. Great results are achieved when the discharge rates, η_1 and η_2 are both steadily decreased to low rates.

Figures 4a-4h show the effects of varying C_h, on both human and bacteria populations when C_e is fixed at low baseline rate of 0.1 and a high efficacy rate of 0.9 respectively. The susceptible population decreases significantly when the direct contact rate, C_h, is high, and decreases even further when paired with low indirect contact rate. However, when the C_e is high, specifically within the range of 0.9 to 1, even with low direct rates, more susceptible individuals become infected with typhoid fever (see figures 4a-4b). Better results are achieved when both indirect contact rate and direct contact rate are sustained at low rates of 0.1. The number of infected

populations is significantly increased with steady increase in direct contact rate, C_h, from 0 to 1 (see figures 4c–4d). The recovered populations, R, is increased with an increase in C_h (see figures 4e–4f). Figures 4g-4h, show that, the bacteria concentration is increased by high rates of C_h. Desirable results are achieved when direct contact rate, C_h and indirect contact rates, C_e are both reduced.

Figures 5a–5h show the effects of varying C_h, on both human and bacteria populations when ψ_f is fixed at low baseline rate of 0.1 and a high efficacy rate of 0.9 respectively. The susceptible population decreases significantly when C_h, is high, and decreases even further when paired with low psychological factor of fear rates. However, when the psychological factor of fear is high, specifically within the range of 0.9 to 1, even with low direct contact rates, fewer susceptible individuals become infected with typhoid fever disease (see figures 5a–5b). Preferable results are achieved when direct contact rate is sustained at low rates and the psychological factor of fear are sustained between 0.9 and 1. The number of infected populations is significantly increased with decrease in psychological factor of fear and high direct contact rates within the range of 0 to 1. However, the infected population is reduced by high rates of the psychological factor of fear and low direct contact rates (see figures 5c–5d). Similarly, recovered populations, R, are reduced with an increase in ψ_f (see figures 5e–5f). Figures 5g-5h, show that, the bacteria concentration is reduced by high rates of ψ_f and low rates of C_h.

Figures 6a–6h show the effects of varying C_h, on both human and bacteria populations when α is fixed at low baseline rate of 0.1 and a high efficacy rate of 0.9 respectively. The susceptible population reduces significantly when the direct contact rate C_h, is high, and decreases even further when coupled with low vaccination rates (see figures 6a–6b). However, when the vaccination aspect is high, specifically within the range of 0.9 to 1, even with low direct contact rates, fewer susceptible individuals become infected with typhoid fever. Better results are attained when vaccination is sustained between 0.9 and 1 and the direct contact rates are low. The number of infected populations is significantly increased with steady increase in direct contact rates, C_h, from 0 to 1 (see figures 6c–6d). Similarly, recovered populations, R, are further

reduced with a decrease in C_h (see figures 6e–6f). Figure 6g–6h, show that, the bacteria concentration is reduced by low rates of C_h. More Suitable results are achieved when direct contact rates, C_h are reduced and vaccination rates, α are steadily increased to high efficacy rates.

Figures 7a–7h show the effects of varying C_e, on both human and bacteria populations when ψ_f is fixed at low baseline rate of 0.1 and a high efficacy rate of 0.9 respectively. The susceptible population reduces significantly with increased indirect contact rates and decreased further when paired with low psychological factor of fear ψ_f (see figures 7a–7b). The infected population is increased by high indirect contact rates and significantly reduced by high rates of psychological factor of fear (see figures 7c–7d). Figures 7e–7f show that, the recovered population significantly increases with increase in indirect contact rate. Figures 7g–7h reveal that the bacteria concentration is reduced by low rates of indirect contact rates and high rates of psychological factor of fear.

Figures 8a–8h show the effects of varying C_e, on both human and bacteria populations when α is fixed at low baseline rate of 0.1 and a high efficacy rate of 0.9 respectively. The susceptible population increases significantly when the indirect contact rate C_e, is high, and increases when paired with low vaccination rates (see figures 8a–8b). However, when the vaccination aspect is high, specifically within the range of 0.9 to 1, even with low indirect rates, fewer susceptible individuals become infected with typhoid fever. Better results are attained when vaccination is sustained between 0.9 and 1 and the indirect contact rate are low. The number of infected populations is significantly increased with steady increase in indirect contact rate, C_e, from 0 to 1 (see figures 8c–8d). Similarly, recovered populations, R, are further reduced with a decrease in C_e (see figures 8e–8f). Figures 8g-8h, show that, the bacteria concentration is reduced by low rates of C_e. Valuable outcomes are achieved when direct contact rates, C_e are reduced and vaccination rates, α is steadily increased to high efficacy rates.

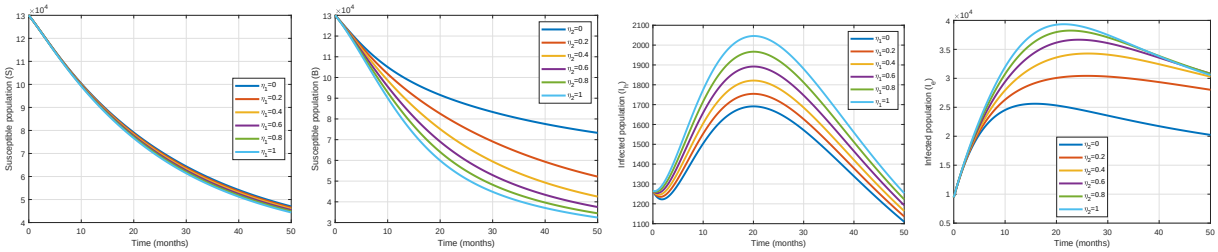

(a) ψ_f and α fixed at 0.5 **(b)** ψ_f and α fixed at 0.5 **(c)** ψ_f and α fixed at 0.5 **(d)** ψ_f and α fixed at 0.5

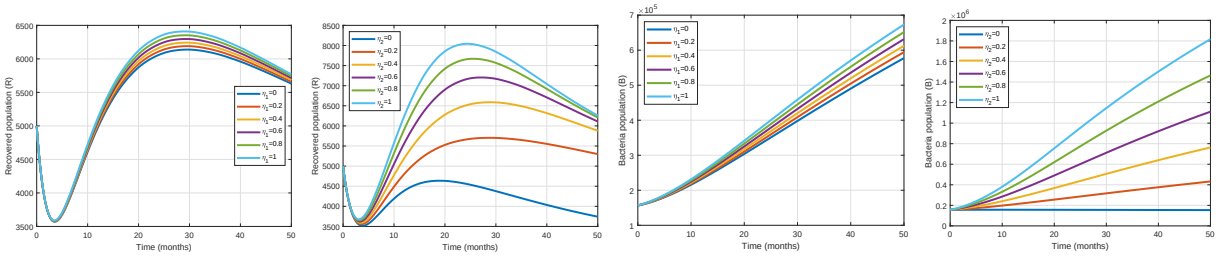

(e) ψ_f and α fixed at 0.5 **(f)** ψ_f and α fixed at 0.5 **(g)** ψ_f and α fixed at 0.5 **(h)** ψ_f and α fixed at 0.5

Figure 3. Effects of Varying η_1 and η_2 when $\alpha = 0.5$ and $\psi_f = 0.5$

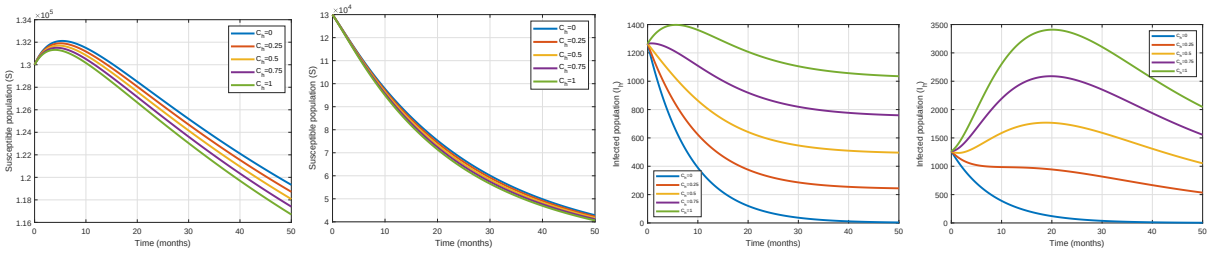

(a) $C_e = 0.1$ **(b)** $C_e = 0.9$ **(c)** $C_e = 0.1$ **(d)** $C_e = 0.9$

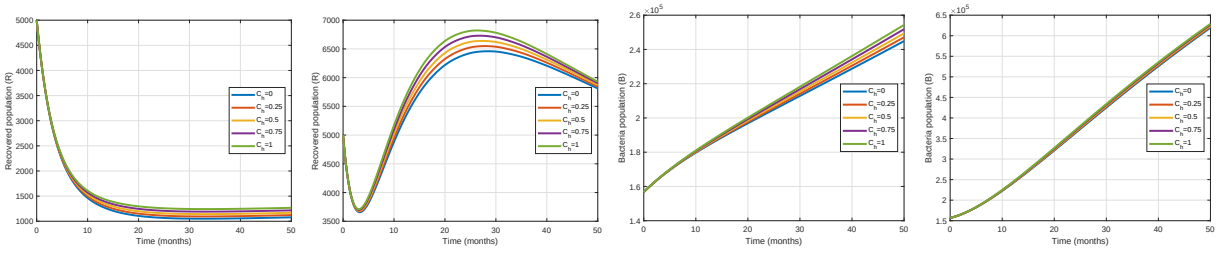

(e) $C_e = 0.1$ **(f)** $C_e = 0.9$ **(g)** $C_e = 0.1$ **(h)** $C_e = 0.9$

Figure 4. Effects of Varying C_h when C_e is fixed at 0.1 and 0.9 respectively

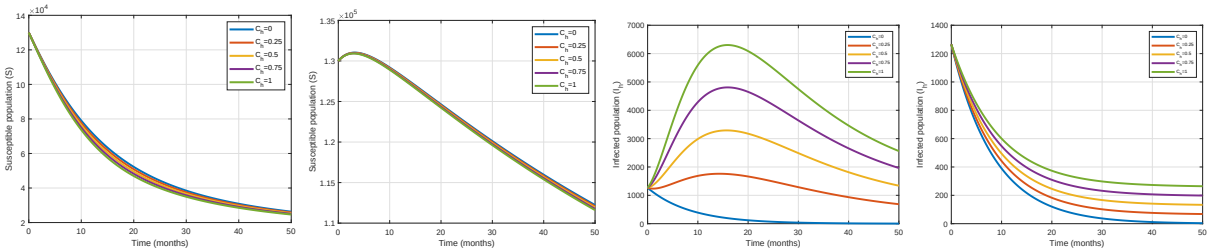

(a) $\psi_f = 0.1$ **(b)** $\psi_f = 0.9$ **(c)** $\psi_f = 0.1$ **(d)** $\psi_f = 0.9$

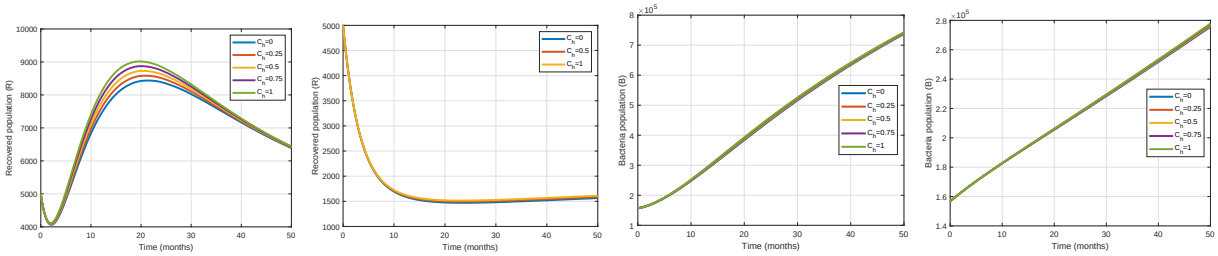

(e) $\psi_f = 0.1$ **(f)** $\psi_f = 0.9$ **(g)** $\psi_f = 0.1$ **(h)** $\psi_f = 0.9$

Figure 5. Effects of Varying C_h when ψ_f is fixed at 0.1 and 0.9 respectively

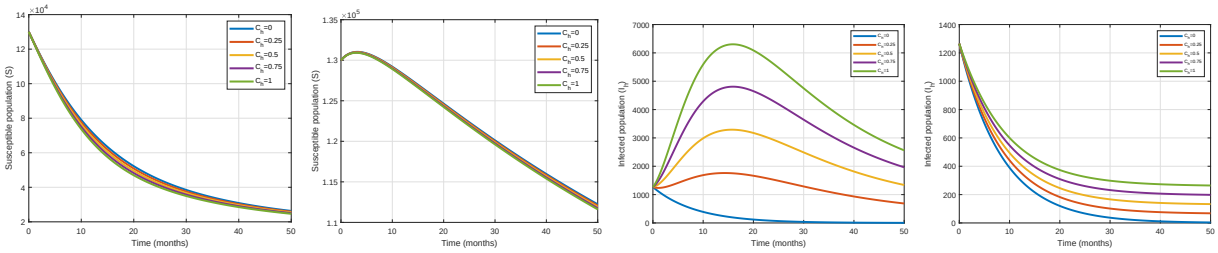

(a) $\alpha = 0.1$ **(b)** $\alpha = 0.9$ **(c)** $\alpha = 0.1$ **(d)** $\alpha = 0.9$

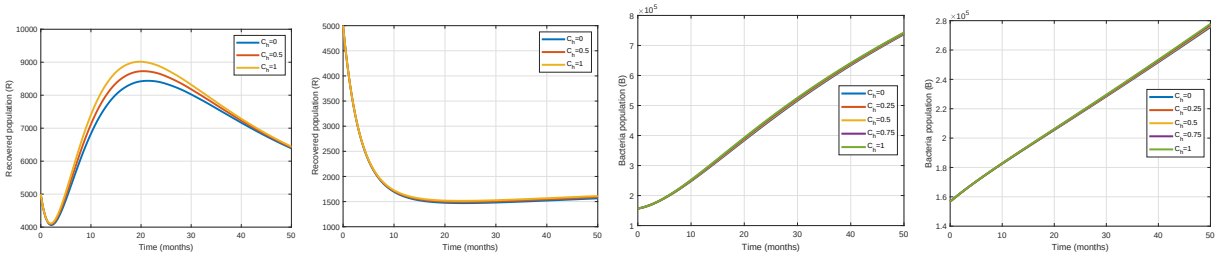

(e) $\alpha = 0.1$ **(f)** $\alpha = 0.9$ **(g)** $\alpha = 0.1$ **(h)** $\alpha = 0.9$

Figure 6. Effects of Varying C_h when α is fixed at 0.1 and 0.9 respectively

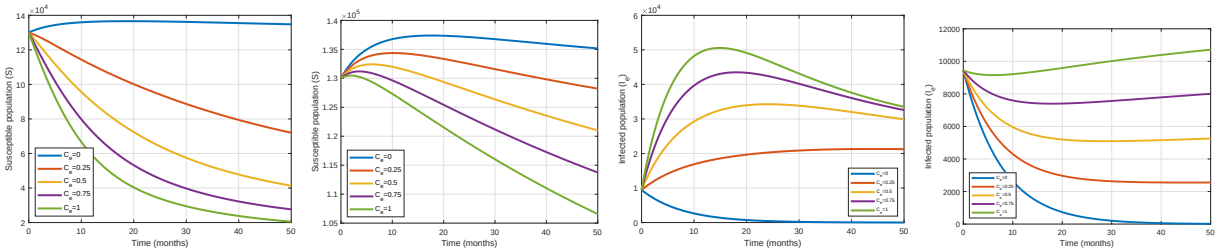

(a) $\psi_f = 0.1$ **(b)** $\psi_f = 0.9$ **(c)** $\psi_f = 0.1$ **(d)** $\psi_f = 0.9$

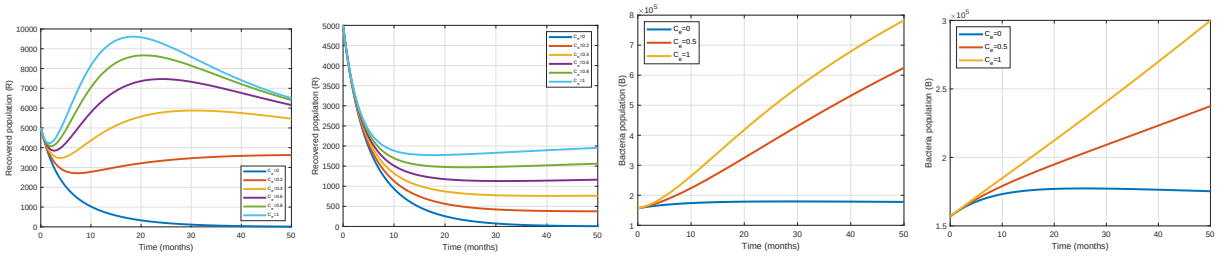

(e) $\psi_f = 0.1$ **(f)** $\psi_f = 0.9$ **(g)** $\psi_f = 0.1$ **(h)** $\psi_f = 0.9$

Figure 7. Effects of Varying C_e when ψ_f is fixed at 0.1 and 0.9 respectively

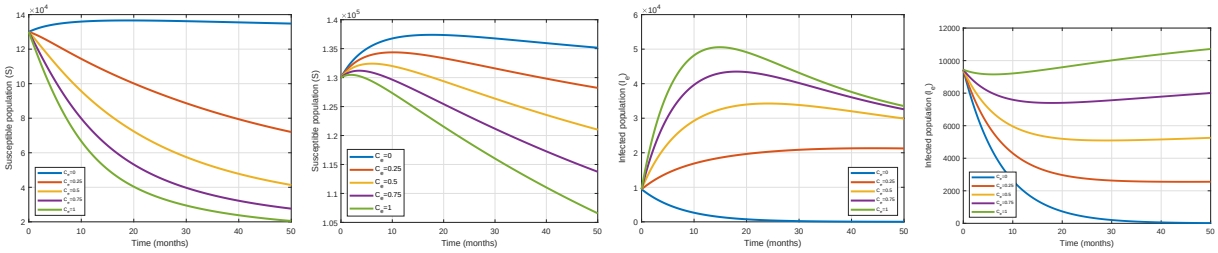

(a) $\alpha = 0.1$ **(b)** $\alpha = 0.9$ **(c)** $\alpha = 0.1$ **(d)** $\alpha = 0.9$

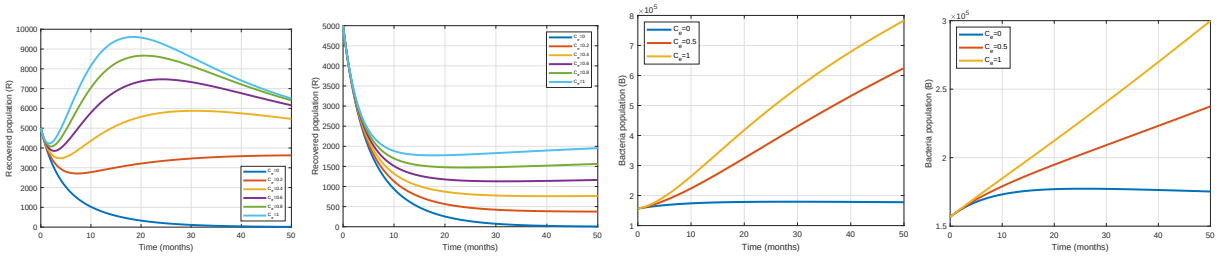

(e) $\alpha = 0.1$ **(f)** $\alpha = 0.9$ **(g)** $\alpha = 0.1$ **(h)** $\alpha = 0.9$

Figure 8. Effects of Varying C_e when α is fixed at 0.1 and 0.9 respectively

5. DISCUSSION

We presented a deterministic model to examine the interplay between human responses driven by the psychological factor of fear of infection and vaccination efforts in the overall transmission dynamics of typhoid fever, while taking into consideration both the direct and indirect modes of transmission. Applying standard mathematical techniques, we studied the qualitative behavior of the deterministic model where we established the feasibility region for the typhoid fever model system, calculated both the disease-free and endemic equilibrium points and determined the necessary conditions for their local and global stability. The typhoid fever model reproduction number $\mathscr{R}_0$ was established using the next generation matrix method and distinct pathways for the transmission of infection were identified, shedding light on the crucial interactions among key population groups fueling the spread of the disease.

Model results show that, heightened psychological factor of fear of typhoid fever disease correlates with a decrease in infection rates. Elevated levels of ψ_f indicate greater self-responsiveness to the disease and fewer infected individuals, thus reducing the pool of potential carriers. This in turn prompts individuals to avoid contaminated water sources, uphold personal hygiene, and ensure proper sanitation, in turn lowering bacterial concentrations in the environment. Further, the model results showed that elevated incidences of typhoid fever correlates with declining immunity post treatment with recovered individuals becoming susceptible to infection, vaccine hesitancy, waning vaccine efficacy on vaccinated populations and reduced psychological factor of fear resulting in less caution when interacting with possible contaminated individuals or environment. Numerical simulations further revealed that indirect mode of transmission was exacerbated by high bacteria concentration in the environment which is replenished by discharge rates from the infected populations. The combined elevated discharge rates increases the infection rate and low sustained discharge rates reduces the transmission rate as shown in Figure 3.

The shedding of the bacteria from the infected classes had a much impact on the bacteria population in the environment. The growth of this bacteria was associated with the significant contribution of *Salmonella Typhi* from the infected humans. From these observations, we deduced that, environmental transmission is associated with the increased discharge rates which

replenish the bacteria concentration. Additionally, avoiding contact with contaminated food and water reduces typhoid fever infection significantly through direct and indirect mode of transmission. Furthermore, when the psychological factor of fear and vaccination rates are sustained at high levels, the contact rate is reduced as shown in Figures (3–8).

Typhoid fever although contained in some parts of Kenya, continues to cause morbidity and mortality particularly to vulnerable informal settlements with low resilience to proper sanitation and safe drinking water with infants and school-aged children most affected. This has resulted in several typhoid fever outbreaks over the recent years. The Kenyan constitution recognizes drinking treated water as a basic human right. From 2010, resource allocation was increased to support water and sanitation access to clean water in the urban informal settlements within Nairobi [4]. In addition, the Government of Kenya made efforts to expand treated water sources, upgrade the piping systems and introduce an aerial water distribution source in a bid to tackle sanitation and reduce transmission of infectious diseases like typhoid fever and cholera [4].

Despite these noble efforts, adequate mitigation efforts to contain typhoid fever in endemic regions continue to face significant hurdles due to poverty, population displacements, inadequate health infrastructure, cultural and religious beliefs, community norms, vaccine hesitancy, insufficient funding to sustain vaccination efforts and adequate infrastructure to support proper sanitation due to government priorities among others. Our model results suggest that increased vaccination efforts particularly safeguards vulnerable populations like infants and school-aged children, owing to the fact they may lack the psychologically capacity to protect themselves from contaminated sources. Numerical simulations further revealed that combined effects of increased vaccination and heightened psychological factor of fear of typhoid fever play a vital role in preventing typhoid fever transmission, resulting in less bacterial shedding into the environment, as shown in Figure 2. In the absence of widespread vaccination against typhoid fever, an increase in the psychological factor of fear of typhoid fever disease is still quite effective in significantly reducing disease transmission in the appropriate demography as shown in this study. The proposed strategies suggested in this study could further support typhoid fever mitigation strategies even in regions with limited resources as self-responsiveness achieves equally good results in containing the disease, even in the absence of vaccination. The proposed model

results will further accelerate the achievement of 2030 Sustainable Development Goal (SDG) aimed at improving health and well-being. Further research could consider the inclusion of demographic aspects such as age and gender, spatial aspects, pathogen detection, pathogen characterization, epidemiological surveillance among others, in the typhoid fever mathematical models.

ACKNOWLEDGMENT

The authors thank the University of Embu for invaluable support and contribution.

DATA AVAILABILITY

The data used to support the findings of this study are included within the article.

CONFLICT OF INTERESTS

The authors declare that there is no conflict of interests.

REFERENCES

[1] T.A. Ayoola, H.O. Edogbanya, O.J. Peter, et al. Modelling and optimal control analysis of typhoid fever, J. Math. Comput. Sci. 11 (2021), 6666-6682. https://doi.org/10.28919/jmcs/6262.

[2] C.L. Kim, L.M. Cruz Espinoza, K.S. Vannice, et al. The burden of typhoid fever in Sub-Saharan Africa: a perspective, Res. Rep. Trop. Med. 13 (2022), 1–9. https://doi.org/10.2147/RRTM.S282461.

[3] S.A. Mina, M.Z. Hasan, A.K.M.Z. Hossain, et al. The prevalence of multi-drug resistant salmonella typhi isolated from blood sample, Microbiol. Insights 16 (2023), 11786361221150760. https://doi.org/10.1177/11786361221150760.

[4] E. Ng'eno, M. Lind, A. Audi, et al. Dynamic incidence of typhoid fever over a 10-year period (2010–2019) in Kibera, an urban informal settlement in Nairobi, Kenya, Amer. J. Trop. Med. Hyg. 109 (2023), 22–31. https://doi.org/10.4269/ajtmh.22-0736.

[5] M. Antillón, J.L. Warren, F.W. Crawford, et al. The burden of typhoid fever in low- and middle-income countries: a meta-regression approach, PLoS Negl. Trop. Dis. 11 (2017), e0005376. https://doi.org/10.1371/journal.pntd.0005376.

[6] D.A. Galgallo, Z.G. Roka, W.G. Boru, et al. Investigation of a typhoid fever epidemic in Moyale Sub-County, Kenya, 2014–2015, J. Health Popul. Nutr. 37 (2018), 14. https://doi.org/10.1186/s41043-018-0144-2.

[7] World Health Organization, Regional Office for Africa, Weekly Bulletin on Outbreak and other Emergencies:Week 17: 17–23 April 2023, World Health Organization, Regional Office for Africa, 2023. https://iris.who.int/handle/10665/367270.

[8] J. Mushanyu, F. Nyabadza, G. Muchatibaya, P. Mafuta, G. Nhawu, Assessing the potential impact of limited public health resources on the spread and control of typhoid, J. Math. Biol. 77 (2018), 647–670. https://doi.org/10.1007/s00285-018-1219-9.

[9] A.D. Steele, M.E. Carey, S. Kumar, et al. Typhoid conjugate vaccines and enteric fever control: where to next?, Clinical Infectious Diseases 71 (2020), S185–S190. https://doi.org/10.1093/cid/ciaa343.

[10] J.E. Meiring, A. Giubilini, J. Savulescu, et al. Generating the evidence for typhoid vaccine introduction: considerations for global disease burden estimates and vaccine testing through human challenge, Clin. Infect. Dis. 69 (2019), S402–S407. https://doi.org/10.1093/cid/ciz630.

[11] A. Addy, Vaccine production and distribution challenges: an AI-assisted technologies for the overcoming of logistical hurdles faced by Sub-Saharan Africa with focus on Ghana, J. Health Med. Nurs. 113 (2024), 33–47. https://doi.org/10.7176/JHMN/113-04.

[12] J.D. Stanaway, P.L. Atuhebwe, S.P. Luby, J.A. Crump, Assessing the feasibility of typhoid elimination, Clin. Infect. Dis. 71 (2020), S179–S184. https://doi.org/10.1093/cid/ciaa585.

[13] S. Edward, A deterministic mathematical model for direct and indirect transmission dynamics of typhoid fever, Open Access Lib. J. 04 (2017), 1–16. https://doi.org/10.4236/oalib.1103493.

[14] L. Matsebula, F. Nyabadza, J. Mushanyu, Mathematical analysis of typhoid fever transmission dynamics with seasonality and fear, Commun. Math. Biol. Neurosci. 2021 (2021), 36. https://doi.org/10.28919/cmbn/5590.

[15] S. Mushayabasa, Modeling the impact of optimal screening on typhoid dynamics, Int. J. Dyn. Control 4 (2016), 330–338. https://doi.org/10.1007/s40435-014-0123-4.

[16] V.V. Volkova, Z. Lu, C. Lanzas, et al. Modelling dynamics of plasmid-gene mediated antimicrobial resistance in enteric bacteria using stochastic differential equations, Sci. Rep. 3 (2013), 2463. https://doi.org/10.1038/srep02463.

[17] F. Verelst, L. Willem, P. Beutels, Behavioural change models for infectious disease transmission: a systematic review (2010–2015), J. R. Soc. Interface 13 (2016), 20160820. https://doi.org/10.1098/rsif.2016.0820.

[18] E. Kanyi, A.S. Afolabi, N.O. Onyango, Mathematical modeling and analysis of transmission dynamics and control of schistosomiasis, J. Appl. Math. 2021 (2021), 6653796. https://doi.org/10.1155/2021/6653796.

[19] L.J.S. Allen, An introduction to mathematical biology, Prentice Hall, 2007. https://cir.nii.ac.jp/crid/1130000796462256768.

[20] C. Castillo-Chávez, Z. Feng, W. Huang, On the computation of R_0 and its role on global stability, in: C. Castillo-Chávez, S. Blower, P. Driessche, et al. (eds) Mathematical approaches for emerging and reemerging infectious diseases: an introduction, vol 125. Springer, Berlin, pp 229–250, (2002).

[21] J.M. Ochoche, R.I. Gweryina, A mathematical model of measles with vaccination and two phases of infectiousness, IOSR J. Math. 10 (2014), 95–105.

[22] M.N. Chamuchi, J.K. Sigey, J.A. Okello, et al. SIICR model and simulation of the effects of carriers on the transmission dynamics of typhoid fever in KISII Town Kenya, SIJ Trans. Comput. Sci. Eng. Appl. 2 (2014), 109–116.

[23] W.O. Alwago, The nexus between health expenditure, life expectancy, and economic growth: ARDL model analysis for Kenya, Reg. Sci. Policy Pract. 15 (2023), 1064–1086. https://doi.org/10.1111/rsp3.12588.

[24] S. Edward, N. Nyerere, Modelling typhoid fever with education, vaccination and treatment, Eng. Math. 1 (2016), 44–52.